Long-Lived MLCT Excited States-Ru^{II} Complexes with a Helical Bis-Phen Ligand

Christine Goze,[a] Jean-Claude Chambron,[a][‡] Valérie Heitz,*[a] Didier Pomeranc,[a] Xavier J. Salom-Roig,[a] Jean-Pierre Sauvage,*[a] Angeles Farrán Morales,[b] and Francesco Barigelletti*[b]

Keywords: Luminescence / N ligands / Photochemistry / Ruthenium

The synthesis of a new Ru^{II} complex [Ru($\mathbf{L_1}$)(4,7-dpphen)]$^{2+}$, bearing a tetradentate bis-1,10-phenanthroline ligand $\mathbf{L_1}$, is described. X-ray crystal structure analysis shows that the tetradentate ligand $\mathbf{L_1}$ coils around the metal and occupies both axial and two of the equatorial positions of the complex. ^{1}H NMR studies clearly indicate that the complex has C_2 symmetry in solution. The room temperature luminescence properties of [Ru($\mathbf{L_1}$)(4,7-dpphen)]$^{2+}$ have been studied, as have those of the related complex [Ru($\mathbf{L_2}$)(4,4′-dmbp)]$^{2+}$. For both complexes, the luminescence quantum yields and lifetimes are three to ten times higher than those of [Ru(bpy)$_3$]$^{2+}$. These unusual results are explained by the geometrical constraints imposed by the tetradentate ligands $\mathbf{L_1}$ and $\mathbf{L_2}$ in their respective complexes, resulting in an effective decoupling between the ^{3}MLCT and ^{3}MC excited states.

Introduction

[Ru(bipy)$_3$]$^{2+}$ (bipy = 2,2′-bipyridine) continues to be the most popular transition metal complex in the field of photochemistry and electron transfer.[1] A huge number of derivatives have been prepared and studied by numerous groups with the improvement of the photochemical properties of Ru-polypyridine complexes in mind, in view of their utilisation in, for instance, molecular photovoltaics and the chemical conversion of light energy.[2,3] In fact, the photochemical stability, the thermal stability of the reduced and oxidized states, the energy levels of the singlet and triplet MLCT states, the emission quantum yield, the ^{3}MLCT excited state lifetime, and the redox properties of the ground and excited states are important parameters that can, to a large extent, be controlled by the structural features of the chelates.[1,4] We now report that, through the use of tetradentate bis-1,10-phenanthroline ligands, which impose a helical geometry to the system in a strictly controlled fashion, the obtained ruthenium(II) complexes display unusually long-lived excited states. This behaviour is probably due to a cage-like effect for the employed tetradentate ligands rather than to electronic delocalisation in their frame systems.

Results and Discussion

The synthesis of [Ru$\mathbf{L_1}$(4,7-dpphen)](PF$_6$)$_2$ is described in Figure 1 (4,7-dpphen represents 4,7-diphenyl-1,10-phenanthroline, as shown in Figure 2). This complex contains the 1,4-phenylenebis(7-bromo-1,10-phenanthroline) ligand $\mathbf{L_1}$, which was synthesized from 7-*p*-bromophenyl-4-methyl-1,10-phenanthroline (**1**). At first, **1** was obtained through a Skraup reaction between 4-methyl-8-aminoquinoline[5,6] and *p*-bromophenyl β-chloroethyl ketone[7] in sulfuric acid in the presence of arsenic pentoxide, in 71% yield.[8] Subsequent treatment of **1** with LDA at −70 °C, followed by addition of α,α′-dibromo-*p*-xylene at −40 °C, afforded $\mathbf{L_1}$ in 7% yield, which is quite low in comparison with a similar reaction producing $\mathbf{L_2}$ in 88% yield.[5,6] This may be due to lower stability of the carbanion of **1**.

Coordination of ligand $\mathbf{L_1}$ on the ruthenium centre was achieved under high-dilution conditions in refluxing dichloroethane with use of [Ru(CH$_3$CN)$_4$Cl$_2$] as precursor complex, as described by von Zelewsky and co-workers.[9] The intermediate complex, [Ru$\mathbf{L_1}$Cl$_2$], formed during the reaction, was treated directly with 4,7-dpphen in a refluxing mixture of water and ethanol. After anion exchange with an aqueous solution of KPF$_6$ and separation by column chromatography, the complex [Ru$\mathbf{L_1}$(4,7-dpphen)](PF$_6$)$_2$

[‡] Present address: Université de Bourgogne, Faculté des Sciences Gabriel, LIMSAG, UMR5633 du CNRS; 6, Boulevard Gabriel; 21100 Dijon, France
[a] Laboratoire de Chimie Organo-Minérale, UMR 7513 du CNRS, Université Louis Pasteur, Faculté de Chimie,
4, rue Blaise Pascal, 67070 Strasbourg Cedex, France
[b] Istituto ISOF-CNR,
Via P. Gobetti 101, 40129 Bologna, Italy

DOI: 10.1002/ejic.200300161

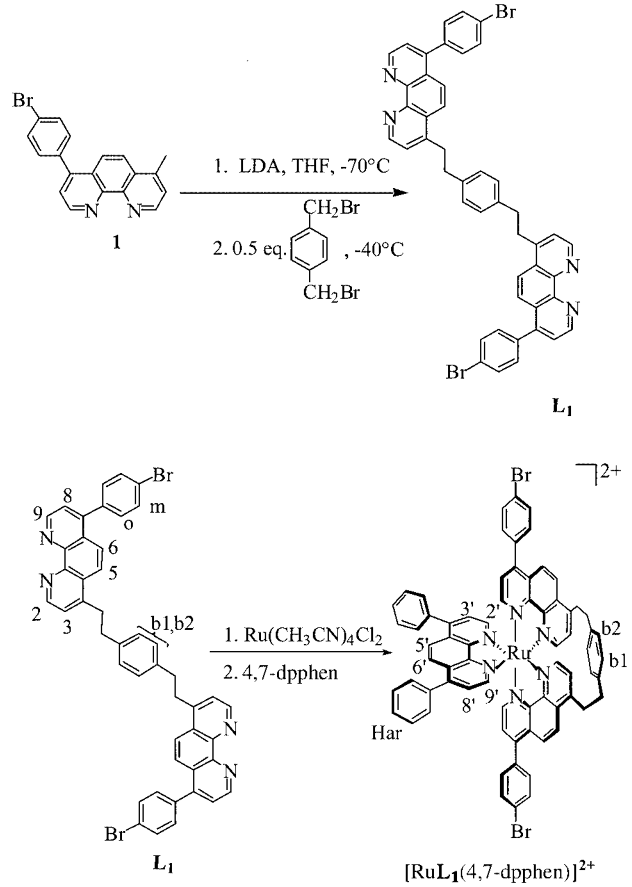

Figure 1. Synthesis of ligand $\mathbf{L_1}$ and preparation of the corresponding ruthenium(II) complex [Ru$\mathbf{L_1}$(4,7-dpphen)]$(PF_6)_2$

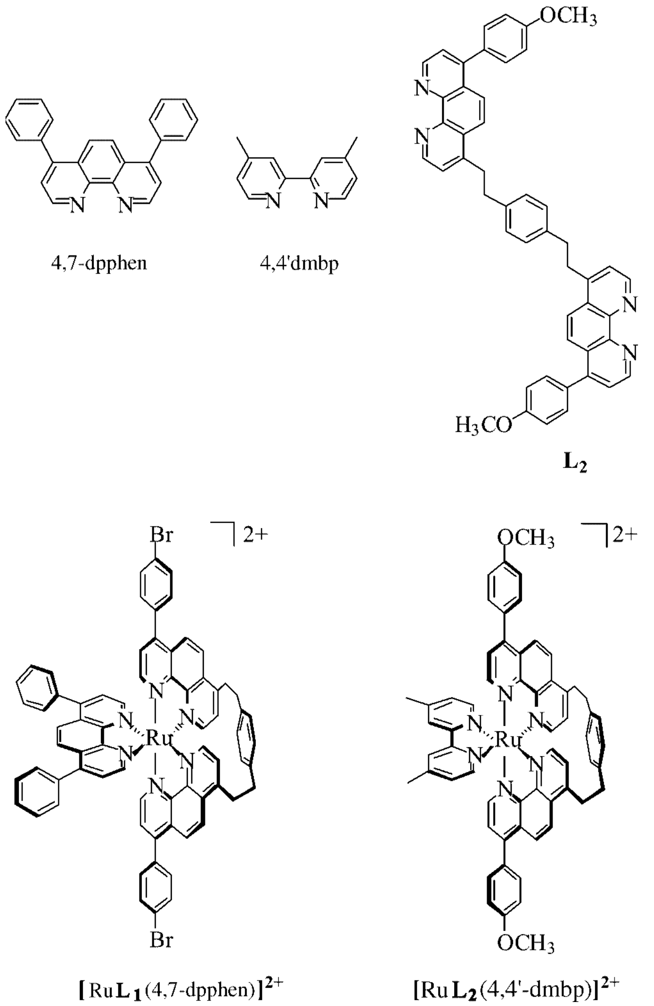

Figure 2. Chemical formulae of the ligands and the complexes studied

was isolated in 44% yield. The C_2 symmetry of the complex in solution is clearly shown by analysis of its ^{1}H NMR spectrum (Figure 3). Protons H^2 and H^9 and protons H^{b1} and H^{b2} of ligand $\mathbf{L_1}$ are particularly sensitive to geometric and electronic changes on going from the free ligand $\mathbf{L_1}$ to the Ru-coordinated ligand $\mathbf{L_1}$ in [Ru$\mathbf{L_1}$(4,7-dpphen)]$(PF_6)_2$, as shown in Figure 3. Protons H^{b1} and H^{b2}, homotopic in $\mathbf{L_1}$ (singlet at $\delta = 7.13$ ppm), become diastereotopic in the C_2 symmetric complex [Ru$\mathbf{L_1}$(4,7-dpphen)]$(PF_6)_2$, appearing as a pair of doublets [$\delta(H^{b1}) = 6.67$ ppm, $\delta(H^{b2}) = 6.32$ ppm]). In the non-coordinated ligand $\mathbf{L_1}$, protons H^2 and H^9 have low-field chemical shifts typical of protons located α to the nitrogen atom of a free 1,10-phenanthroline [$\delta(H^2) = 9.04$ ppm and $\delta(H^9) = 9.19$ ppm]. These protons are shifted upfield in the complex [$\delta(H^2) = 7.39$ ppm and $\delta(H^9) = 7.99$ ppm], since coiling of the ligand around the ruthenium centre places H^2 in the shielding field of the other phenanthroline of $\mathbf{L_1}$ and H^9 in that of the ancillary ligand 4,7-dpphen.

The X-ray crystal structure of the complex [Ru$\mathbf{L_1}$(4,7-dpphen)]$(PF_6)_2$ was solved (Figure 4).[10] The complex crystallises in the monoclinic *P*12/n1 space group, with two molecules in the unit cell. The structure clearly shows that the axial and two equatorial positions are occupied by the nitrogen atoms of the ligand $\mathbf{L_1}$ and that the remaining equatorial positions are occupied by the 4,7-dpphen ligand. The Ru−N distances range between 2.057(9) Å and 2.076(9) Å. This structure is close to that of the complex [Ru$\mathbf{L_2}$(4,4′-dmbp)]$(PF_6)_2$,[5] but with less distortion from linearity. The angle Br(1)−Ru−Br(2) is 174.6(9)°, as compared with 169.9(7)° for O−Ru−O. The distance Br(1)···Br(2) is 21.86(8) Å.

The synthesis of the ruthenium complex [Ru$\mathbf{L_2}$(4,4′-dmbp)]$(PF_6)_2$ has been described previously.[5,6] This complex contains a bis-1,10-phenanthroline ligand $\mathbf{L_2}$, functionalized with a *p*-anisyl group on each position 7 of the phenanthroline unit (Figure 2), and differs from the former mainly in the nature of the ancillary ligand [4,4′-dimethyl-2,2′-bipyridine (4,4′-dmbp)].

Figure 5 shows the absorption spectra ($1\cdot10^{-5}$ M, acetonitrile) of the investigated complexes containing the tetradentate ligands $\mathbf{L_1}$ and $\mathbf{L_2}$; for purposes of comparison, the spectrum of [Ru(bpy)$_3$]$(PF_6)_2$ is also shown.

For the [Ru$\mathbf{L_2}$(4,4′-dmbp)]$(PF_6)_2$ and [Ru$\mathbf{L_1}$(4,7-dpphen)]$(PF_6)_2$ complexes, the lowest-lying ^{1}MLCT band maxima fall at slightly lower energies − 458 and 460 nm, respectively − than that of the reference complex [Ru-

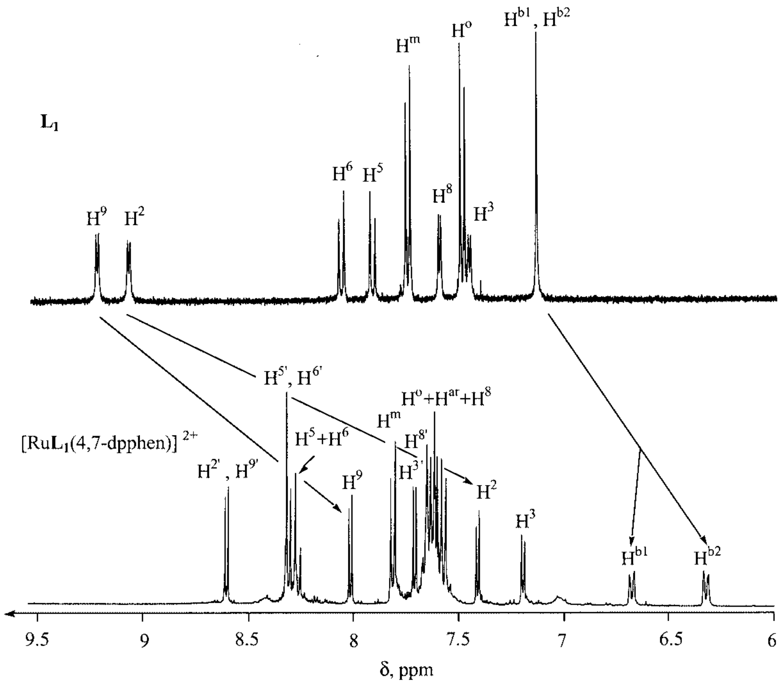

Figure 3. 400 MHz ^{1}H NMR spectra (low field region, CD_2Cl_2) of ligand **L$_1$** and complex [Ru**L$_1$**(4,7-dpphen)]$(PF_6)_2$

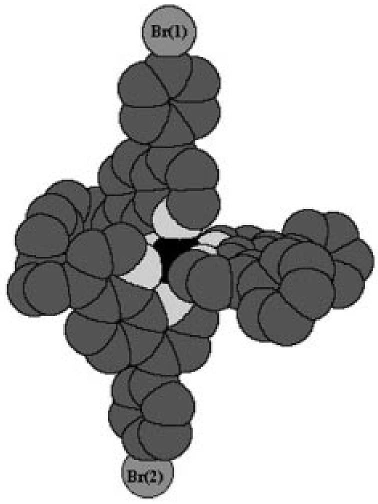

Figure 4. X-ray crystal structure of [Ru**L$_1$**(4,7-dpphen)]$(PF_6)_2$

$(bpy)_3](PF_6)_2$ (452 nm). The absorption intensities at the MLCT band maxima are ε = 20300 and 20600 $\text{M}^{-1}\cdot\text{cm}^{-1}$, respectively, and hence about 40% higher than that of the reference complex (ε = 14300 $\text{M}^{-1}\cdot\text{cm}^{-1}$). This is an effect due to the "transfer term" for the promoted electron,[11−13] the average displacement of which during the MLCT transition is larger than that occurring in the case of $[Ru(bpy)_3]^{2+}$. The MLCT absorption features for [Ru**L$_2$**(4,4′-dmbp)]$(PF_6)_2$ and [Ru**L$_1$**(4,7-dpphen)]$(PF_6)_2$ thus suggest that the MLCT transitions in the visible region probably involve the extended frames of the **L$_2$** and **L$_1$** ligands, respectively {and also of the ligand 4,7-dpphen in the case of [Ru**L$_1$**(4,7-dpphen)]$(PF_6)_2$}.

An observation of interest relates to the presence of intense absorption bands appearing at 310−320 nm for [Ru**L$_2$**(4,4′-dmbp)]$(PF_6)_2$ and [Ru**L$_1$**(4,7-dpphen)]$(PF_6)_2$, but not exhibited by $[Ru(bpy)_3](PF_6)_2$ (see Figure 5). This is a spectral region in which ^{1}MC (d-d) transitions are expected for Ru^{II}-polypyridine complexes.[1] This type of transition is Laporte-forbidden, and its extinction coefficient is estimated ε ≈ 10^2 $\text{M}^{-1}\cdot\text{cm}^{-1}$ for $[Ru(bpy)_3]^{2+}$.[14] The fact that for [Ru**L$_1$**(4,7-dpphen)]$(PF_6)_2$ and − even more so − for [Ru**L$_2$**(4,4′-dmbp)]$(PF_6)_2$, the forbidden nature of the transition appears to be substantially lifted may be associated with permanent or transient distortions of the octahedral environment around the metal centre; the X-ray results (see above) are consistent with this interpretation. Finally, the absorption features in the 280−290 nm spectral portion are ^{1}LC in nature and are probably attributable to the ligand subunits directly coordinated to the metal centre,[1] as shown by the fact that their intensities are similar; see Figure 5.

Room temperature luminescence properties of [Ru**L$_2$**(4,4′-dmbp)]$(PF_6)_2$ and [Ru**L$_1$**(4,7-dpphen)]$(PF_6)_2$, obtained in degassed acetonitrile, are illustrated in Table 1; for purposes of comparison, luminescence results for $[Ru(bpy)_3](PF_6)_2$ are also listed.

The room temperature luminescence profiles (shown in the inset of Figure 5), the band peaks and the lifetime values are consistent with a ^{3}MLCT nature for the lowest-lying level of the investigated Ru-polypyridine luminophores. The band maxima of [Ru**L$_2$**(4,4′-dmbp)]$(PF_6)_2$ and [Ru**L$_1$**(4,7-dpphen)]$(PF_6)_2$ are slightly lower in energy than that of $[Ru(bpy)_3](PF_6)_2$, consistently with the absorption results. The relevant observation here is that, for the two complexes containing the tetradentate ligands **L$_1$** and **L$_2$**, the lumi-

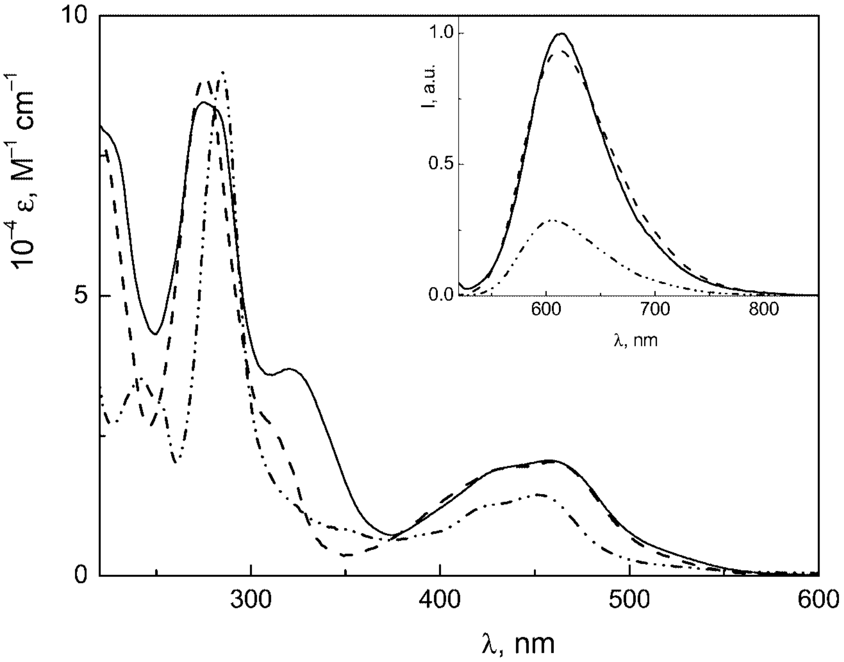

Figure 5. Ground state absorption spectra in acetonitrile for $[RuL_2(4,4'\text{-dmbp})](PF_6)_2$ (full line), $[RuL_1(4,7\text{-dpphen})](PF_6)_2$ (dash), and $[Ru(bpy)_3](PF_6)_2$ (dash-dot-dot); the inset shows luminescence spectra obtained from excitation of isoabsorbing solutions at 450 nm

Table 1. Luminescence properties (O_2-free acetonitrile solvent, excitation at 450 or 337 nm)

	298 K					77 K	
	λ_{max}, nm	φ	τ, μs	$k_r \times 10^4$, s^{-1}[a]	$k_{nr} \times 10^5$, s^{-1}[b]	λ_{max}, nm	τ, μs
$[RuL_2(4,4'\text{-dmbp})](PF_6)_2$	614	0.30	4.0	7.5	1.8	608	10.5
$[RuL_1(4,7\text{-dpphen})](PF_6)_2$	612	0.28	8.6	3.3	0.83	610	11.2
$[Ru(bpy)_3](PF_6)_2$	608	0.086	0.90	9.6	10.2	585	4.9

[a] $k_r = \varphi / \tau$. [b] $k_{nr} = (1 - \varphi)/\tau$.

nescence quantum yields (Φ) and lifetimes (τ) are three to ten times larger than those for $[Ru(bpy)_3](PF_6)_2$. In these complexes, this happens because the non-radiative transitions (as quantified by the appropriate rate constant k_{nr}; see Table 1), known to govern the luminescence properties in the Ru-polypyridine complexes,[1,4] appear to be substantially depressed. Below we briefly discuss possible reasons for this behaviour.

With regard to the nature of the non-radiative processes deactivating the ^{3}MLCT luminescent level in Ru-polypyridine complexes, three main issues can be considered. These are: (i) the effect of the electronic delocalisation in the ligand system,[13,15,16] (ii) the effect of the energy gap law (regarding the direct ^{3}MLCT-to-GS transition),[17,18] and (iii) the thermal accessibility from the luminescent ^{3}MLCT level of a higher-lying ^{3}MC state, an effective doorway both to photochemistry (ligand release) and to fast, non-radiative deactivation (because of the strong ^{3}MC-GS coupling).[1] Given the extended ligand systems of L_1 and L_2, and also of 4,7-dpphen, we have addressed the role of electronic delocalisation, point (i), in detail. The extent of delocalisation is related to the displacement of the potential energy curve for the luminescent MLCT excited state with respect to the curve for the ground state (GS) (i.e., a high degree of delocalisation is accompanied by a small displacement). Analysis of the luminescence profiles affords the displacement parameter, the Huang−Rys electron-vibrational coupling constants pertinent to average frequencies (S_M) of ligand origin, $\hbar\omega_M = 1350$ cm^{-1}, corresponding to the vibrational progression exhibited by the low-temperature luminescence spectra.[15,16] The results of the vibronic analysis on the corrected luminescence profiles (on an energy scale, spectra obtained in frozen solvent at 77 K) are illustrated in Figure 6 and summarized in Table 2.

While for complexes containing highly delocalised ligand systems, such as dipyrido-phenazine,[19] pyrimidine-substituted terpyridine (tpy)[20] or back-to-back bis-tpy,[13] this type of vibronic analysis provides S_M values of between 0.2 and 0.5, for $[RuL_2(4,4'\text{-dmbp})](PF_6)_2$ and $[RuL_1(4,7\text{-dpphen})](PF_6)_2$ we find $S_M = 0.75$ and 0.78 (Table 2). These values are not greatly different from that for $[Ru(bpy)_3](PF_6)_2$ ($S_M = 0.92$) taken as a prototype of a complex in which the ligand system is not greatly delocalised. The vibronic analysis does not therefore support delocalisation

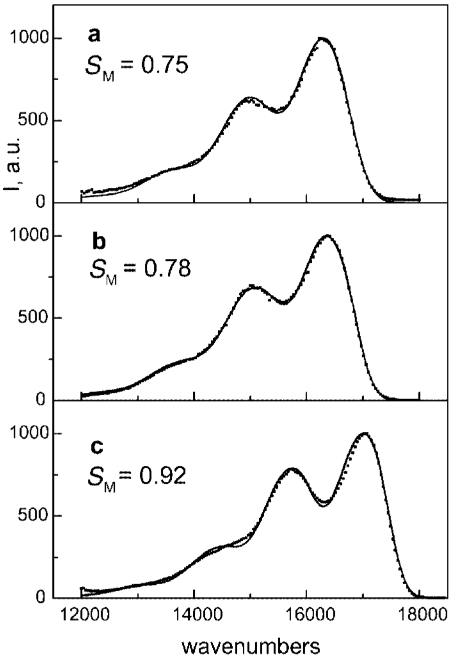

Figure 6. Vibronic analysis of the luminescence profiles for $[\mathrm{Ru}\mathbf{L}_1(\text{4,7-dpphen})](\mathrm{PF}_6)_2$ (**a**), $[\mathrm{Ru}\mathbf{L}_2(\text{4,4}'\text{-dmbp})](\mathrm{PF}_6)_2$ (**b**), and $[\mathrm{Ru(bpy)}_3](\mathrm{PF}_6)_2$ (**c**), obtained at 77 K, acetonitrile, excitation at 450 nm; see text for further details

Table 2. Parameters from vibronic analysis (from fitting of the 77 K luminescence profiles, Equation (2) of text)

	E_{00}, cm^{-1} [a]	S_M [b]
$[\mathrm{Ru}\mathbf{L}_2(\text{4,4}'\text{-dmbp})](\mathrm{PF}_6)_2$	16680	0.78
$[\mathrm{Ru}\mathbf{L}_1(\text{4,7-dpphen})](\mathrm{PF}_6)_2$	16540	0.75
$[\mathrm{Ru(bpy)}_3](\mathrm{PF}_6)_2$	17250	0.92

[a] Energy of the luminescent level (0−0 transition). [b] Huang−Rys factor for frequencies of ligand origin, $\hbar\omega_M$ = 1350 cm^{-1}.

in the ligands as a crucial factor for explaining the quite different luminescence features of $[\mathrm{Ru}\mathbf{L}_2(\text{4,4}'\text{-dmbp})](\mathrm{PF}_6)_2$ and $[\mathrm{Ru}\mathbf{L}_1(\text{4,7-dpphen})](\mathrm{PF}_6)_2$, in comparison with the case of $[\mathrm{Ru(bpy)}_3](\mathrm{PF}_6)_2$. Effects related to point (ii) above (energy-gap law)[17,18] would also be expected to be of limited importance, given that the luminescent levels are not too apart from one another in energy (Table 2). In conclusion, we point to the fact that the tetradentate **L**$_1$ and **L**$_2$ ligands contain two bidentate subunits linked together. Literature examples exist in which constraints against elongation of the Ru−N bonds (inhibiting ligand release as a consequence of extreme elongation) can result in a sort of cage-like effect; this type of restrictions can originate from physical interactions, as found within zeolite frameworks, for instance,[21] or can be imposed at the molecular level by linking the coordinating bpy units together, thus yielding caged or hemi-caged complexes.[22] For the luminescent levels of both the $[\mathrm{Ru}\mathbf{L}_2(\text{4,4}'\text{-dmbp})](\mathrm{PF}_6)_2$ and the $[\mathrm{Ru}\mathbf{L}_1(\text{4,7-dpphen})](\mathrm{PF}_6)_2$ complexes, the reduced role of the non-radiative relaxation is probably related to such a cage-type effect, due to coordination of the tetradentate **L**$_1$ and **L**$_2$ ligands.

In conclusion, we have been able to show that the use of a bis-phen ligand, displaying geometrically constraining properties with respect to the coordination sphere of the complexed ruthenium(II) centre, produces effective decoupling between the ^{3}MLCT and the ^{3}MC excited states. This effect results in remarkably long-lived ^{3}MLCT excited states for the corresponding ruthenium(II)-tris(diimine) complexes.

Experimental Section

Materials: Starting materials were from commercial sources and were used as received. THF was distilled from sodium/benzophenone prior to use. Reactions performed under an atmosphere of argon used standard Schlenk techniques. $[\mathrm{Ru(CH_3CN)_4Cl_2}]$ was prepared according to the literature procedure.[9]

Physical Measurements: ^{1}H NMR: Bruker WP200SY (2OOMHz) and Bruker AM (400 MHz) instruments; the reported chemical shifts are referenced to $\mathrm{Me_4Si}$ as an internal standard. Mass spectroscopic data were obtained on a ZAB-HF (FAB) spectrometer with a nitrobenzyl alcohol matrix.

7-(*p*-Bromophenyl)-4-methyl-1,10-phenanthroline (1): A mixture of 4-methylquinolin-8-ylamine (1.5 g, 9.5 mmol), arsenic acid (5.65 g, 13.3 mmol), and phosphoric acid (15 mL) was heated at 100 °C. *p*-Bromophenyl-β-chloroethylketone[7] (3.28 g, 13.3 mmol) was added over a period of 1 h at such a rate that the temperature did not exceed 120 °C. After the addition the temperature was raised to 140 °C for 2 hours. After cooling, the mixture was poured onto ice and the resulting solution was neutralised with aqueous sodium hydroxide (30%), resulting in the precipitation of a brown solid. The mixture was left at 0 °C overnight. The precipitate was extracted several times with boiling toluene, the combined solutions were dried with $\mathrm{MgSO_4}$, and the solvent was evaporated. The crude product was chromatographed on silica, eluted with hexane/ethyl acetate (50:50), with a gradient to ethyl acetate/methanol (99:1), yielding **1** as a pale brown solid (2.34 g, 71%). ^{1}H NMR (200 MHz, $\mathrm{CDCl_3}$): δ = 2.78 (s, 3 H, $\mathrm{CH_3}$), 7.42 (d, ^3J = 8.12 Hz, 2 H, H^m), 7.49 (d, ^3J = 4.42 Hz, 1 H, H^3), 7.53 (d, ^3J = 4.42 Hz, 1 H, H^8), 7.70 (d, ^3J = 8.12 Hz, 2 H, H^o), 7.86 (d, ^3J = 9.34 Hz, 1 H, H^5), 7.97 (d, ^3J = 9.36 Hz, 1 H, H^6), 9.07 (d, ^3J = 4.42 Hz, 1 H, H^2), 9.22 (d, ^3J = 4.42 Hz, 1 H, H^9) ppm. FAB-MS: *m*/*z* = 349.4 $[\mathrm{M + H}]^+$.

L$_1$: Diisopropylamine (0.162 mL, 1.15 mmol) was dissolved in THF (4 mL) under argon. *n*-Butyllithium (1.5 M, 0.764 mL) was added at 0 °C, and the mixture was stirred at 0 °C for 1 h. Compound **1** (400 mg, 1.15 mmol) was dissolved in THF (10 mL) under argon and transferred by cannula at −40 °C to the freshly prepared LDA solution. The solution instantly turned dark red and was stirred for 1 hour at −70 °C and for 1/2 h at −40 °C. α,α′-Dibromo-*p*-xylene (151.2 mg, 0.057 mmol) was dissolved in THF (5 mL) under argon and transferred to the reaction mixture at −40 °C by cannula. The mixture was stirred at room temperature overnight, during which the dark red solution turned pale brown. The solution was poured into water and extracted with dichloromethane. The combined organic phases were washed with ethanol in order to remove the oligomers and chromatographed on alumina, eluted with dichloromethane with a gradient to dichloromethane/methanol (98:2), to yield **L**$_1$ as a brown solid (32 mg, 7%). ^{1}H

NMR (400 MHz, CD_2Cl_2): δ = 3.09 (m, 4 H, CH_2), 3.42 (m, 4 H, CH_2), 7.13 (s, 4 H, $H^{b1}+H^{b2}$), 7.44 (d, ^3J = 4.20 Hz, 2 H, H^3), 7.47 (d, ^3J = 8.25 Hz, 4 H, H^o), 7.58 (d, ^3J = 4.39 Hz, 2 H, H^8), 7.73 (d, ^3J = 8.22 Hz, 4 H, H^m), 7.90 (d, ^3J = 9.37 Hz, 2 H, H^5), 8.05 (d, ^3J = 9.43 Hz, 2 H, H^6), 9.04 (d, ^3J = 4.32 Hz, 2 H, H^2), 9.19 (d, ^3J = 4.35 Hz, 2 H, H^9) ppm. FAB MS: *m/z* = 801 [M + H]$^+$.

[RuL$_1$(4,7-dpphen)](PF$_6$)$_2$: Compound **L$_1$** (50 mg, 0.062 mmol) was dissolved in 1,2-dichloroethane (15 mL) under argon. Freshly prepared $[Ru(CH_3CN)_4Cl_2]$ (21 mg, 0.062 mmol) was dissolved in 1,2-dichloroethane (15 mL) under argon. The two solutions were simultaneously added dropwise to refluxing 1,2-dichloroethane (800 mL) at a rate of 5 mL/h. After completion of the addition, the dark violet mixture was heated at reflux for two more hours, and allowed to cool overnight. The solvent was evaporated, and the resulting dark violet solid was dissolved in a mixture of ethanol/water (8 mL/1 mL) under argon. 4,7-Diphenylphenanthroline (4,7-dpphen, 20.6 mg, 0.062 mmol) was then added, and the reaction mixture was heated for 4 h, during which the solution turned orange-red. After the mixture had cooled, the ethanol was evaporated and the product was precipitated with a saturated aqueous solution of potassium hexafluorophosphate. The resulting precipitate was filtered under vacuum and chromatographed on silica, eluting with a gradient of dichloromethane/methanol, from 100:0 to 90:10. The complex [RuL$_1$(4,7-dpphen)](PF_6)$_2$ was obtained as an orange solid (41 mg, 44%). TLC: one spot, R_f = 0.62 (CH_2Cl_2/MeOH, 8:2). ^{1}H NMR (400 MHz, CD_2Cl_2): δ = 3.11 (m, 2 H, CH_2), 3.28 (m, 2 H, CH_2), 3.42 (m, 2 H, CH_2), 3.94 (m, 2 H, CH_2), 6.32 (dd, ^3J = 7.95, ^4J = 1.6 Hz, 2 H, H^{b2}), 6.67 (dd, ^3J = 8.07, ^4J = 1.72 Hz, 2 H, H^{b1}), 7.18 (d, ^3J = 5.36 Hz, 2 H, H^3), 7.39 (d, ^3J = 5.4 Hz, 2 H, H^2), 7.55 (d, ^3J = 8.52 Hz, 4 H, H^o), 7.59 (d, ^3J = 5.5 Hz, 2 H, H^8), 7.61 (m, 10 H, H^{ar}), 7.68 (d, ^3J = 5.52 Hz, 2 H, $H^{3',8'}$), 7.79 (d, ^3J = 8.52 Hz, 4 H, H^m), 7.99 (d, ^3J = 5.4 Hz, 2 H, H^9), 8.24 (d, ^3J = 9.32 Hz, 2 H, H^5), 8.28 (d, ^3J = 9.2 Hz, 2 H, H^6), 8.29 (s, 2 H, $H^{5',6'}$), 8.57 (d, ^3J = 5.52 Hz, 2 H, $H^{2',9'}$) ppm. FAB MS: *m/z* = 1379.1 [M − PF_6^-]$^+$, 1234.2 [M − 2PF_6^- + e^-]$^+$, 617.6 [M − 2PF_6^-]$^{2+}$/2.

Optical Spectroscopy: Absorption spectra were recorded with a Perkin−Elmer Lambda 9 spectrophotometer in dilute (10^{-5} M) acetonitrile solutions. Luminescence experiments were performed in pump-freeze-thaw degassed acetonitrile at room temperature and at 77 K (liquid nitrogen temperature, samples were in capillary tubes immersed in a quartz finger Dewar).

Luminescence spectra were obtained with a Spex Fluorolog II spectrofluorimeter equipped with a Hamamatsu R928 phototube. Uncorrected luminescence band maxima are used throughout the text unless otherwise stated; in order to determine luminescence quantum yields and to perform the vibronic analyses (see below) of luminescence intensity profiles, we employed corrected luminescence spectra on an energy scale (cm^{-1}). The corrected spectra were obtained either by use of a correction curve provided by the supplier or by employment of a calibrated 45-W quartz-halogen tungsten filament lamp (Optronic Laboratories) as a standard for the correction of the phototube response. Luminescence quantum yields Φ_s were obtained according to Equation (1),[23] where *s* and *r* stand for sample and reference standard, respectively, A is the absorbance (taken ≤ 0.1) at the selected excitation wavelength, and n is the refractive index of the solvent. $[Ru(bpy)_3]Cl_2$ was chosen as a reference standard (Φ = $2.8\cdot10^{-2}$ in air-equilibrated water).[24] The experimental uncertainty in the band maximum for absorption and luminescence spectra is 2 nm; that for luminescence quantum yield is 20%. Luminescence lifetimes were obtained with an IBH single-photon-counting apparatus (N_2 lamp, excitation at 337 nm). The uncertainty in the evaluated lifetimes is 8%.

$$\frac{\Phi_s}{\Phi_r} = \frac{A_r n_s^2 (area)_s}{A_s n_r^2 (area)_r} \tag{1}$$

Vibronic band intensities of the luminescence spectra on an energy scale (cm^{-1}) were analysed according to a fitting procedure proposed by Meyer and co-workers.[25,26] For the luminescence spectra obtained at 77 K we used a two-mode analysis according to the following expression [Equation (2)]:

$$I(\bar{v}) = \sum_{v_M=0}^{\infty}\sum_{v_L=0}^{\infty} \left(\frac{\bar{v}_{oo} - v_M\bar{v} - v_L\bar{v}}{\bar{v}_{oo}}\right)^3 \left(\frac{S_M^{v_M}}{v_M!}\right) \times \left(\frac{S_L^{v_L}}{v_M!}\right) \exp\left[-(4\ln 2)\left(\frac{\bar{v} - \bar{v}_{oo} - v_M\bar{v} - v_L\bar{v}}{\bar{v}_{1/2}}\right)^2\right] \tag{2}$$

where $I(\bar{v})$ is the luminescence intensity profile, $\bar{v}_\infty$ is the energy of the 0−0 transition (hereafter indicated as E_∞), *v* are vibrational quantum numbers, *M* and *L* are labels for average and low frequency modes, taken as $\hbar\omega_M$ = 1350 cm^{-1} and $\hbar\omega_M$ = 400 cm^{-1}, respectively, S_M and S_L are displacement parameters along the indicated vibrational modes, and $\bar{v}_{1/2}$ is the bandwidth at half maximum (fwhm) of the vibronic line.

Acknowledgments

Thanks are due to the EU for financial support (A. F. M., TMR contract CT98-0226), and to Prof. T. J. Meyer and D. J. P. Claude for kindly providing the software for the vibronic analysis. X. J. S. R. thanks the Rectorat de l'Université Louis Pasteur for financial support. D. P. thanks the French Ministry of education for a fellowship.

---

[1] A. Juris, V. Balzani, F. Barigelletti, S. Campagna, P. Belser, A. von Zelewsky, *Coord. Chem. Rev.* **1988**, *84*, 85−277.

[2] C. A. Bignozzi, J. R. Schoonover, F. Scandola, *Molecular Level Artificial Photosynthetic Materials* **1997**, *44*, 1−95.

[3] J. K. McCusker, *Science* **2001**, *293*, 1599−1601.

[4] J.-P. Sauvage, J.-P. Collin, J.-C. Chambron, S. Guillerez, C. Coudret, V. Balzani, F. Barigelletti, L. De Cola, L. Flamigni, *Chem. Rev.* **1994**, *94*, 993−1019.

[5] D. Pomeranc, V. Heitz, J.-C. Chambron, J.-P. Sauvage, *J. Am. Chem. Soc.* **2001**, *123*, 12215−12221.

[6] D. Pomeranc, J.-C. Chambron, V. Heitz, J.-P. Sauvage, *Comptes Rendus Acad. Sci. Ser. II C* **2001**, *4*, 197−200.

[7] F. G. Bordwell, W. T. Brannen, Jr., *J. Am. Chem. Soc.* **1964**, *86*, 4645−4650.

[8] F. H. Case, *J. Chem. Soci.* **1951**, 1541−1545.

[9] P. Hayoz, A. von Zelewsky, H. Stoeckli-Evans, *J. Am. Chem. Soc.* **1993**, *115*, 5111−5114.

[10] Summary of data: formula: $C_{78}H_{60}Br_2F_{12}N_{10}P_2Ru_1$. Unit cell parameters: *a:* 13.0677(1), *b:* 15.3308(3), *c:* 20.3461(3) Å; beta: 100.641(5)°. Space group *P2/n*. CCDC-201524 contains the supplementary crystallographic data for this paper. These data can be obtained free of charge at www.ccdc.cam.ac.uk/conts/retrieving.html [or from the Cambridge Crystallographic Data

Centre, 12, Union Road, Cambridge CB2 1EZ, UK; Fax: (internat.) +44-1223/336-033; E-mail: deposit@ccdc.cam.ac.uk].

[11] P. Day, N. Sanders, *J. Chem. Soc., A* **1967**, 1536.

[12] L. De Cola, F. Barigelletti, *Inorg. Chim. Acta* **1989**, *159*, 169.

[13] L. Hammarström, F. Barigelletti, L. Flamigni, M. T. Indelli, N. Armaroli, G. Calogero, M. Guardigli, A. Sour, J.-P. Collin, J.-P. Sauvage, *J. Phys. Chem. A* **1997**, *101*, 9061−9069.

[14] D. M. Roundhill, *Photochemistry and Photophysics of Metal Complexes*, Plenum Press, New York, **1994**, Ch. 5.

[15] J. A. Treadway, B. Loeb, R. Lopez, P. A. Anderson, F. R. Keene, T. J. Meyer, *Inorg. Chem.* **1996**, *35*, 2242−2246.

[16] G. F. Strouse, J. R. Schoonover, R. Duesing, S. Boyde, W. E. Jones, T. J. Meyer, *Inorg. Chem.* **1995**, *34*, 473−487.

[17] J. V. Caspar, E. M. Kober, B. P. Sullivan, T. J. Meyer, *J. Am. Chem. Soc.* **1982**, *104*, 630.

[18] R. Englman, J. Jortner, *Mol. Phys.* **1970**, *18*, 145.

[19] J. A. Treadway, G. F. Strouse, R. R. Ruminski, T. J. Meyer, *Inorg. Chem.* **2001**, *40*, 4508−4509.

[20] Y. Q. Fang, N. J. Taylor, G. S. Hanan, F. Loiseau, R. Passalacqua, S. Campagna, H. Nierengarten, A. Van Dorsselaer, *J. Am. Chem. Soc.* **2002**, *124*, 7912−7913.

[21] K. Maruszewski, J. R. Kincaid, *Inorg. Chem.* **1995**, *34*, 2002−2006.

[22] F. Barigelletti, L. De Cola, V. Balzani, P. Belser, A. von Zelewsky, F. Vögtle, F. Ebmeyer, S. Grammenudi, *J. Am. Chem. Soc.* **1989**, *111*, 4662−4668.

[23] J. N. Demas, G. A. Crosby, *J. Phys. Chem.* **1971**, *75*, 991.

[24] K. Nakamaru, *Bull. Chem. Soc., Jpn.* **1982**, *55*, 2967.

[25] J. P. Claude, T. J. Meyer, *J. Phys. Chem.* **1995**, *99*, 51−54.

[26] K. R. Barqawi, Z. Murtaza, T. J. Meyer, *J. Phys. Chem.* **1991**, *95*, 47−50.

Received March 27, 2003